Characteristics of Anthropogenic Pollution in the Atmospheric Air of South-Western Svalbard (Hornsund, Spring 2019)

Filip Pawlak [1], Krystyna Koziol [2], Wanda Wilczyńska-Michalik [3], Mikołaj Worosz [4,†], Marek Michalik [4], Sara Lehmann-Konera [5] and Żaneta Polkowska [1,*]

[1] Department of Analytical Chemistry, Chemical Faculty, Gdańsk University of Technology, 80-233 Gdańsk, Poland; filpawla@pg.edu.pl
[2] Department of Environmental Change and Geochemistry, Faculty of Geographical Sciences, Kazimierz Wielki University in Bydgoszcz, 85-033 Bydgoszcz, Poland; krykozio@ukw.edu.pl
[3] Polish Geophysical Society (PTGeof.), 00-927 Warsaw, Poland; wanda.michalik@post.pl
[4] Institute of Geological Sciences, Jagiellonian University, 30-387 Cracow, Poland; marek.michalik@uj.edu.pl (M.M.)
[5] Institute of Earth and Environmental Sciences, Faculty of Earth Sciences and Spatial Management, Maria Curie-Skłodowska University in Lublin, 20-718 Lublin, Poland; sara.lehmann-konera@mail.umcs.pl
* Correspondence: zanpolko@pg.edu.pl
† MSc student.

Supporting Information

S1. Materials and methods 3

Table S1. Analytical parameters. 3

Table S2. Temperature program. 4

Table S3. Mass/charge ration and retention time. 4

Table S4. Validation parameters such as recovery, coefficient of variation (CV) for ten samples with known POP content, limit of detection (LOD) and limit of quantification (LOQ). 5

S2.1. POP concentrations 7

Table S5. The content of seven PCBs in atmospheric air [pg/m^3] 7

Table S6. Content of selected organochlorine pesticides in atmospheric air [pg/m^3] 7

S2.2 Additional interpretation factors: sea ice situation during the sampling period ... 8

Figure S1. Sea ice situation on May 6th in the area surrounding Svalbard. 9

S2.3 Meteorological conditions and backward air mass trajectories 9

Figure S2. Air mass trajectories arriving at Hornsund during each of the sample collections (labeled with the last day of sampling). 10

Figure S3. Precipitation (bars) and average air temperature (dots) measured at the PPSH station in April and May 2019..... 11

S3. Study limitations 11

S1. Materials and methods

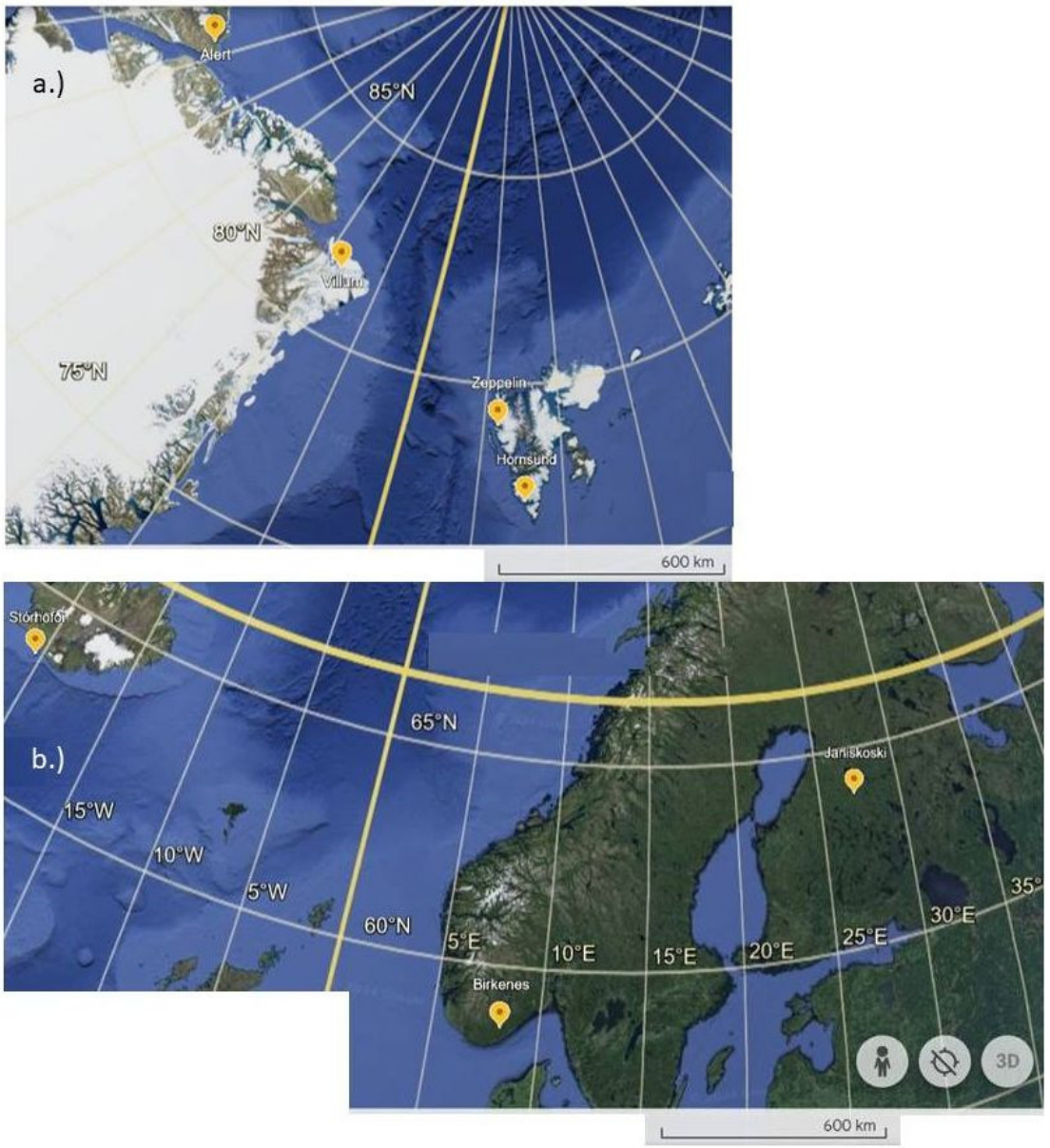


Figure S1. Map of the relative location of the compared air monitoring stations within the Arctic: a.) northern part, b.) southern part. Background: Google Earth.

Table S1. Analytical parameters

Analytes	Reagents/Standards/Equipment	Analytical technique	Measurement instrumentation/ Analysis conditions	
Organochlorine pesticides (OCPs)[b] Dichlorodiphenyldichloroethylene (DDE) Dichlorodiphenyltrichloroethane (DDT) Dichlorodiphenyldichloroethane (DDD) Hexachlorocyclohexane (α-, β-, and γ HCH) Heptachlor epoxide Aldrin	Hexane and acetone, isooctane (HPLC-grade) (MERCK, Darmstadt, Germany); Pesticide standards from single-compound solutions: α-HCH, γ-HCH, heptachlor epoxide, 2,4'-DDD, 4,4'-DDD, 2,4'-DDE, 4,4'-DDE, 2,4'-DDT, 4,4'-DDT (all: 100 mg mL^{-1} in cyclohexane), β-HCH (100 mg/L in toluene) Aldrin (100 mg mL^{-1} in isooctane), LGC standards, London, UK) Certified isotope-labeled standard: 4,4'-DDT-d8 (100 µg mL^{-1} in acetone, Dr Ehrenstorfer™, LGC Group, North Charleston, United States)	Gas chromatography coupled with triple-quadrupole mass spectrometry (GC-MS/MS)	Gas chromatograph (8890 GC System, Agilent Technologies) coupled with a triple-quadrupole mass spectrometer (7010 B, Agilent Technologies CA, USA)	Detector (Agilent Technologies 5975C) with electron ionization (EI), detector working mode: dynamic multiple reaction monitoring mode (dMRM*); autosampler (MultiPurposeSampler MPS robotic pro XL—GERSTEL); column: HP5-MS (5% phenyl-methylpolysiloxane, 30 m × 250 µm × 0.25 µm); solvent delay: 6 min; injection volume: 5 µL (splitless), inlet temperature: 300 ˚C, carried gas: helium (1 mL min^{-1}), collision gas: N_2 (1.5 mL min^{-1}), quench gas: He (2.5 mL min^{-1})
Polychlorinated biphenyls (PCBs)[b] PCB 05, 11, 28, 52, 101, 118, 138, 169, 153, and 180	Hexane and acetone, isooctane (HPLC-grade) (MERCK, Darmstadt, Germany); PCB standards, IUPAC No. 28, 52, 101, 118, 138, 153, 180 (10 mg mL^{-1} in isooctane; Dr Ehrenstorfer™; LGC Group, North Charleston, United States); Certified isotope-labeled standards: PCB 28 ($^{13}C_{12}$, 99%), PCB 180 ($^{13}C_{12}$, 99%), (40 mg mL^{-1} in nonane), Cambridge Isotope Laboratories, Tewksbury, MA, USA			

Table S2. Temperature program

	Rate [^{o}C min^{-1}]	Value [^{o}C]	Hold Time [min]	Run Time [min]
Initial		40	2	2
Ramp 1	25	150	0	5.2
Ramp 2	3	200	0	21.9
Ramp 3	8	280	10	41.9
Ramp 4	100	300	5	47.1
Post Rune		300	15	62.1

Table S3. Mass/charge ratio and retention time.

Compound Name	Precursor Ion	Product Ion	RT	Left RT delta	Right RT delta	CE (eV)
α-HCH	218.9	183		1	2	5
α-HCH	216.9	181	12.90	1	2	5
α-HCH	180.9	145		1	2	15
β-HCH	218.9	183.1		1	2	5
β-HCH	216.9	181.1	13.90	1	2	5
β-HCH	181	145		1	2	15
γ-HCH	219	183.1		1	2	5
γ-HCH	217	181.1	14.20	1	2	5
γ-HCH	181.1	145.1		1	2	15
PCB 28	258	186		2	2	25
PCB 28	256	186	16.90	2	2	25
PCB 28	186	151		2	2	25
PCB 28 isotopically labeled	268	198.1	17.00	2	2	25
PCB 52	291.9	221.9		2	2	25
PCB 52	289.9	219.9	18.70	2	2	25
PCB 52	255	220		2	2	10
PCB 101	253.9	184		2	2	35
PCB 101	325.9	255.9	23.96	2	2	35
PCB 101	327.9	255.9		2	2	35
Aldrin	262.9	192.9		2	2	35
Aldrin	262.9	190.9	19.35	2	2	35
Aldrin	254.9	220		2	2	20
Heptachlor epoxide	354.8	264.9		2	2	15
Heptachlor epoxide	352.8	316.8	21.50	2	2	5
Heptachlor epoxide	352.8	262.9		2	2	15

o,p'-DDE	317.8	248		2.04	2	15
o,p'-DDE	248	176.2	23.00	2.04	2	30
o,p'-DDE	246	176.2		2.04	2	30
o,p'-DDD	235	200.1		2	2	10
o,p'-DDD	235	165.1	24.50	2	2	25
o,p'-DDD	199.1	164.1		2	2	20
p,p'-DDD	237	200.1		2	2	15
p,p'-DDD	237	165.1	24.50	2	2	25
p,p'-DDD	165.1	115		2	2	35
p,p'-DDE	317.8	246		2	3	15
p,p'-DDE	315.8	246	24.50	2	3	15
p,p'-DDE	246.1	176.2		2	3	30
PCB 118	325.9	255.9		2	2	30
PCB 118	325.9	253.9	25.70	2	2	30
PCB 118	253.9	184		2	2	35
p,p'-DDT	237	165.2		2.5	2.5	20
p,p'-DDT	235	199.2	26.10	2.5	2.5	15
p,p'-DDT	235	165.2		2.5	2.5	20
o,p'-DDT	237	165.2		2	2	20
o,p'-DDT	235	199.1	26.13	2	2	15
o,p'-DDT	235	165.2		2	2	20
PCB 138	359.9	324.9		2	2	15
PCB 138	359.9	289.9	26.40	2	2	30
PCB 138	287.9	217.9		2	2	40
p,p'-DDT isotopically labeled	243	173.1	27.19	1	1	35
PCB 153	361.9	289.9		2	2	25
PCB 153	359.9	289.9	27.30	2	2	25
PCB 153	287.9	217.9		2	2	40
PCB 180	395.8	323.8		2	2	30
PCB 180	393.8	358.8	29.30	2	2	15
PCB 180	393.8	323.8		2	2	30
PCB 180 isotopically labeled	406	335.8	29.40	2	2	25

Table S4. Validation parameters such as recovery, coefficient of variation (CV) for ten samples with known POP content, limit of detection (LOD) and limit of quantification (LOQ).

	LOD [ng]	LOQ [ng]	CV	Recovery %
α-HCH	0.004	0.012	2.7	106.9
β-HCH	0.035	0.105	0.74	105.08
γ-HCH	0.025	0.07525	0.55	103.72
Aldrin	0.016	0.0475	2.4	124.3

Heptachlor epoxide	0.025	0.075	0.94	125.94
DDD	0.043	0.125	0.8	119.1
o.p'-DDE	0.0083	0.0245	0.069	117.669
p.p'-DDE	0.050	0.15	0.61	125.26
o.p'-DDT	0.012	0.038	0.56	116.27
p.p'-DDT	0.017	0.05	3.6	109.2
PCB 28	0.0028	0.008	0.51	89.83
PCB 52	0.0045	0.013	0.98	65.03
PCB 101	0.040	0.12	0.81	68.38
PCB 118	0.028	0.085	2.4	72.4
PCB 138	0.021	0.0623	1.6	78.1
PCB 153	0.040	0.12	0.67	76.49
PCB 180	0.065	0.19	0.48	77.3
PCB 28 isotopically labeled	-	-	1	100
p.p'-DDT isotopically labeled	-	-	1.6	85.9
PCB 180 isotopically labeled	-	-	2.1	108.8

From blank sample analyses, the limit of detection (LOD) was calculated, using the following formula:

(1) $LOD = S + 3.3\sigma$,

where S = mean value for 10 replicates and σ = standard deviation for these replicates.

The limit of quantification (LOQ) was then calculated as follows:

(2) $LOQ = 3 \times LOD$.

S1.1 Hybrid Single-Particle Lagrangian Integrated Trajectory (HYSPLIT)

The analysis of directions of the inflow of air masses employed the NOAA Air Resources Lab HYSPLIT Trajectories model (Lehmann-Konera et al., 2024; Rolph et al., 2017; Stein et al., 2015). The model verified backward trajectories of air masses for each sampled period, for three elevations: a HYSPLIT-generated mid-boundary layer height, 500 m and 1000 m above mean sea level. At 12:00 UTC on the specified measurement day, using the relevant GDAS Meteorological Data and wind speed, along with the Model Vertical Velocity, the vertical movement of air masses was simulated. These trajectories allow us to ascertain where pollutants entering the study area within a specific timeframe originated from. However, it is important to note that these trajectories do not

definitively pinpoint the sources of pollutants, and they do not exclude the possibility of air masses coming from other regions. The intricate nature of atmospheric circulation processes results in errors within these trajectories, which become more pronounced as the backward forecast duration increases. To mitigate this, a 72-hour period was chosen.

S2. Results and discussion

S2.1. POP concentrations

Table S5. The content of seven PCBs in atmospheric air [pg/m^3].

Sampling periods in 2019		A1 (17 -24.04)	A2 (24.04- 02.05)	A3 (02-11.05)
Air volumes	[m^3]	1226.605	1208.989	1519.722
Analytes				
PCB-28	AV	0.347	0.868	<LOD
	SD	0.046	0.01	-
PCB-52	AV	0.113	0.42	<LOD
	SD	0.028	0.13	-
PCB-101	AV	<LOD	<LOD	<LOD
	SD	-	-	-
PCB-118	AV	<LOD	0.3143	<LOD
	SD	-	0.0055	-
PCB-138	AV	<LOD	0.029	<LOD
	SD	-	0.036	-
PCB-153	AV	<LOD	0.632	<LOD
	SD	-	0.029	-
PCB-180	AV	<LOD	<LOD	<LOD
	SD	-	-	-

Table S6. Content of selected organochlorine pesticides in atmospheric air [pg/m^3].

Sampling periods in 2019		A1 (17 -24.04)	A2 (24.04 - 02.05)	A3 (02- 11.05)
Air volumes	[m^3]	1227	1209	1519
Analytes				
α-HCH	AV	17.4	29.8	28.1
	SD	1.2	0.35	0.038
β-HCH	AV	0.777	2.76	0.179
	SD	0.0064	0.088	0.063
γ-HCH	AV	22.5	68.4	26.8
	SD	3.9	1.7	0.65
Aldrin	AV	2.94	19.6	28.3
	SD	0.13	1.2	0.036

Heptachlor epoxide	AV	0.379	0.398	0.283
	SD	0.012	0.0026	0.012
DDD	AV	<LOD	9.83	1.89
	SD	-	0.097	0.086
o.p'-DDE	AV	1.59	3.75	1.60
	SD	0.32	0.051	0.044
p.p'-DDE	AV	12.6	10.5	8.35
	SD	1.5	0.059	0.34
o.p'-DDT	AV	<LOD	<LOD	<LOD
	SD	-	-	-
p.p'-DDT	AV	5.52	2.83	2.41
	SD	0.16	0.022	0.045

S2.2 Additional interpretation factors: sea ice situation during the sampling period

The sea ice coverage during the sampling period was very consistent, with very close drift ice covering the north-western Greenland Sea together with most of the Fram Strait, the Arctic Ocean north of Svalbard and the Barents Sea directly to the east from Svalbard. The only brief change within the one-month fieldwork period was the sea ice becoming slightly less close in the Greenland Sea and part of the Barents Sea on 6th-7th May. Combined with air mass backward trajectories, such a situation implicated the passing of air masses incoming to Hornsund over sea ice for half of the sampling period ending 24th April 2019 (the northern trajectories), most of the time within the sampling period ending 2nd May 2019 (only selected stretches of trajectories south of Svalbard passing over the open sea) and during the entire sampling period ending on 11th May 2019.

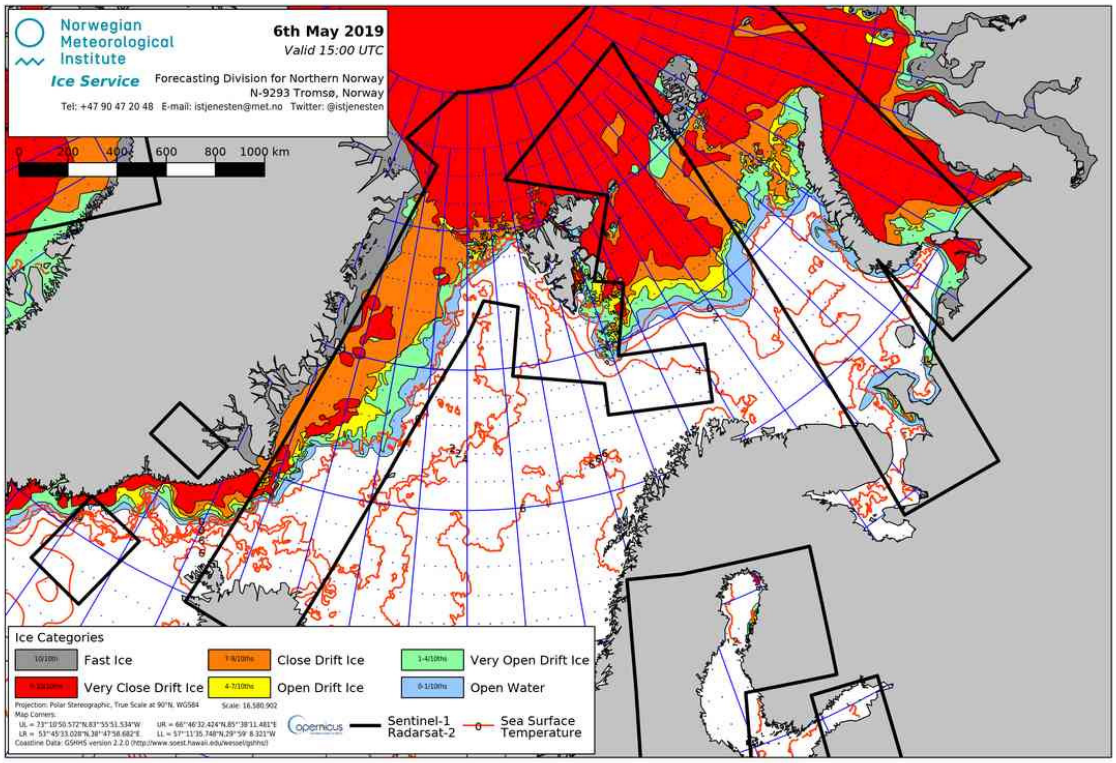


Figure S2. Sea ice situation on May 6th in the area surrounding Svalbard. Source: Norwegian Meteorological Institute, Ice Service: https://cryo.met.no/archive/ice-service/icecharts/quicklooks/.

S2.3 Meteorological conditions and backward air mass trajectories

The first period between April 14th and 24th (Figures S3.A,B,C) began with an influx of warm air masses coming from the south (western Norway, northern British Isles), lasting until April 20th, causing temperatures above zero and precipitation. A change of direction followed, bringing air masses from the north (northern coasts of Greenland, Canada and the central Arctic Ocean) and a drop in temperature (Figure S4). No precipitation was observed at that time, and this episode lasted until about April 25th, ending within the period covering the collection of the second air sample. During the second period, which started on April 24th and lasted until May 2th (Figures S3.D, E, F), there was also a warmer stage, with an influx of air from the Greenland, Barents and Norwegian seas and a slight precipitation at the end (until April 29th). The last and longest weather pattern started on April 29th and lasted until May 11th (Figures S3. G, H, I). During this event, there was no precipitation, the temperature

oscillated around -5°C and the air masses came from the north-east (northern coast of Russia, eastern part of the Arctic Ocean).

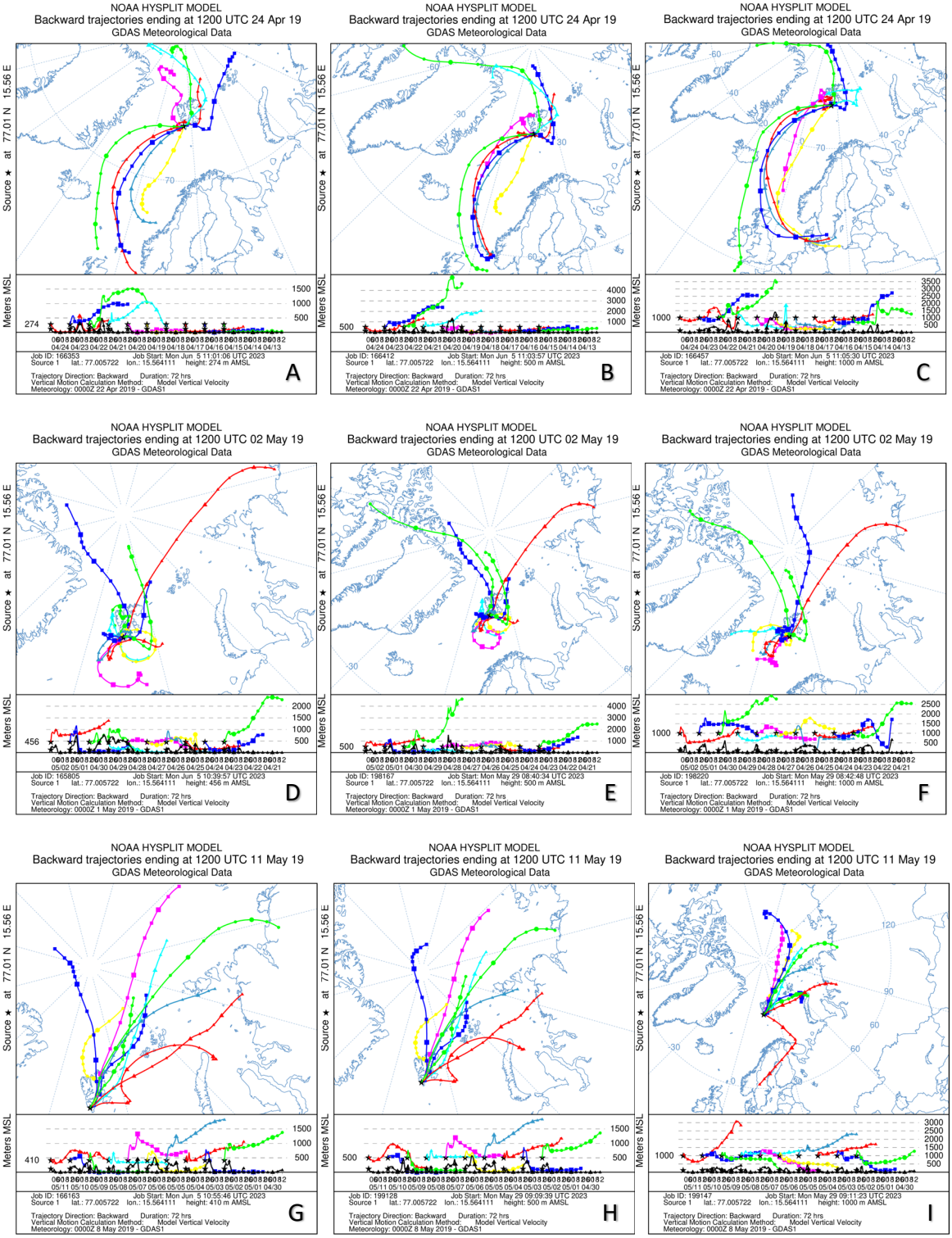


Figure S3. Air mass trajectories arriving at Hornsund during each of the sample collections (labeled with the last day of sampling): left—automatic mid-boundary layer height; middle—500 m above mean sea level (AMSL); right—1000 m AMSL.

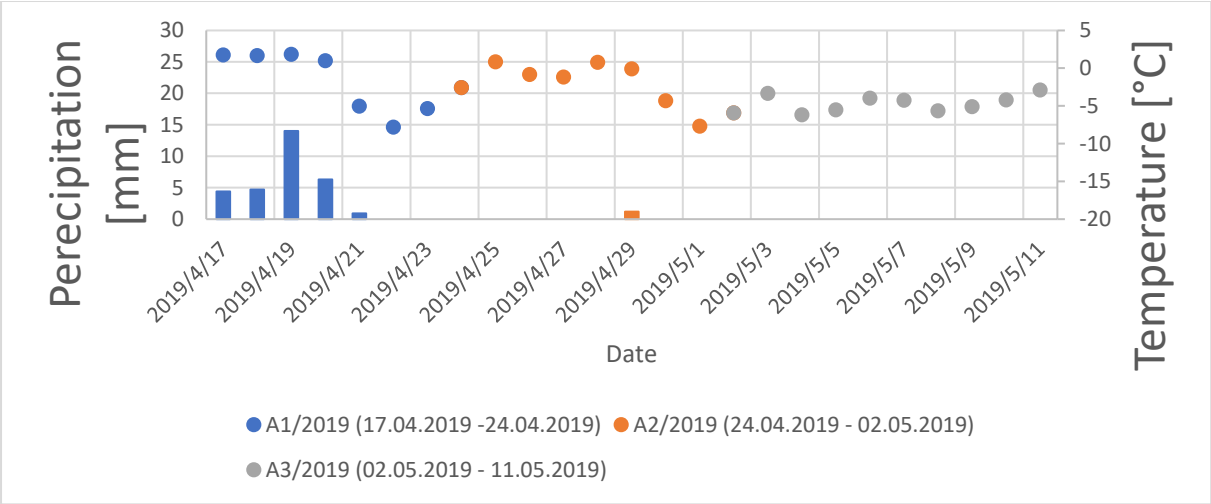


Figure S4. Precipitation (bars) and average air temperature (dots) measured at the PPSH station in April and May 2019.

References quoted in SM

Bossi, R., Vorkamp, K., Skov, H., 2016. Concentrations of organochlorine pesticides, polybrominated diphenyl ethers and perfluorinated compounds in the atmosphere of North Greenland. Environ. Pollut. 217, 4–10. https://doi.org/10.1016/j.envpol.2015.12.026

Choël, M., Deboudt, K., Flament, P., 2010. Development of time-resolved description of aerosol properties at the particle scale during an episode of industrial pollution plume. Water. Air. Soil Pollut. 209, 93–107. https://doi.org/10.1007/s11270-009-0183-9

Lehmann-Konera, S., Marek Ruman, Marcin Frankowski, Łukasz Małarzewski, Krzysztof Raczyński, Filip Pawlak, Joanna Jóźwik, Joanna Potapowicz, and Żaneta Polkowska. 2024. "Short-Term Observations of Rainfall Chemistry Composition in Bellsund (SW Spitsbergen, Svalbard)" *Water* 16, no. 2: 299. https://doi.org/10.3390/w16020299

Rolph, G., Stein, A., Stunder, B., 2017. Real-time Environmental Applications and Display sYstem: READY. Environ. Model. Softw. 95, 210–228. https://doi.org/10.1016/j.envsoft.2017.06.025

Stein, A.F., Draxler, R.R., Rolph, G.D., Stunder, B.J.B., Cohen, M.D., Ngan, F., 2015. NOAA's HYSPLIT Atmospheric Transport and Dispersion Modeling System. Bull. Am. Meteorol. Soc. 96, 2059–2077. https://doi.org/10.1175/BAMS-D-14-00110.1